Biochem. J. (1991) 277, 231–238 (Printed in Great Britain)

Assembly of chick brain MAP2–tubulin microtubule protein

Characterization of the protein and the MAP2-dependent addition of tubulin dimers

Roy G. BURNS
Biophysics Section, Blackett Laboratory, Imperial College of Science, Technology and Medicine, London SW7 2BZ, U.K.

The principle proteins present in twice-cycled chick brain microtubule protein were characterized. The protein consists of a stoichiometric mixture of MAP2 and tubulin, together with a number of minor components. Its composition remains unaltered after a third cycle of assembly in a buffer supplemented with 67 mM-NaCl, with the exception of the phosphorylation of MAP2 to a low level ($\simeq 1$ mol·mol^{-1}). The inclusion of 67 mM-NaCl dissociates the MAP2–tubulin oligomers, and restricts the assembly to the MAP2-dependent addition and loss of tubulin dimers, such that the assembly kinetics approximate to a simple pseudo-first-order reaction. The assembled microtubules exhibit dynamic instability, with no evidence for end-to-end annealing.

INTRODUCTION

The analysis of microtubule assembly *in vitro* has contributed significantly to an understanding of the behaviour of microtubules *in vivo*. These *in vitro* studies have increasingly concentrated on analysing the assembly of pure tubulin, yet there is widespread evidence for the co-localization of microtubule-associated proteins (MAPs) *in vivo*, and that the MAPs can affect kinetic properties *in vitro* (see, e.g., Murphy *et al.*, 1977; Bré & Karsenti, 1990). Our aim has therefore been to characterize the assembly kinetics of microtubule protein, containing a stoichiometric mixture of tubulin and the dendritic MAP2, in order to investigate the regulatory mechanisms effected by MAP2.

The first detailed study of the kinetics of microtubule assembly (Johnson & Borisy, 1977) showed that the addition and loss of 'subunits' to a microtubule end conform to the predictions of a simple linear condensation model, i.e.:

$$-\mathrm{d[Tu]}/\mathrm{d}t = k_{+1}{}^{GTP}[\mathrm{Tu}^{GTP}][\mathrm{M}] - k_{-1}{}^{GTP}[\mathrm{M}]$$

(the various terms are defined in the abbreviations footnote). Various developments restrict the validity of this simple model.

(*a*) The different critical concentrations of the two microtubule ends, leading to the property termed "treadmilling" (Margolis & Wilson, 1978) or "head-to-tail polymerisation" (Cote & Borisy, 1981).

(*b*) Brain tubulin is highly heterogeneous, resulting from the transcription of multiple α- and β-tubulin genes (Cleveland & Sullivan, 1985) and post-translational additions including tyrosinylation (Arce & Barra, 1983), acetylation (Piperno & Fuller, 1985), Ca^{2+}/calmodulin-dependent phosphorylation (Wandosell *et al.*, 1986) and glutamylation (Eddé *et al.*, 1990) and their respective removals. Equilibrium models cannot apply if there is selective use of specific isotypes or if the assembly conditions alter the extent of the post-translational modifications.

(*c*) Microtubule proteins from a variety of sources contain single and double gyre rings [see, e.g., Erickson, 1974; Kirschner *et al.*, 1974; Scheele & Borisy, 1978), which partially dissociate on warming and which may be directly incorporated into an elongating microtubule (Pantaloni *et al.*, 1981; Bordas *et al.*, 1983; Bayley *et al.*, 1985), rendering it difficult to define the concentration of free subunits and hence to calculate the association rate constant. One approach to eliminate such oligomer involvement has been to centrifuge the protein immediately before assembly (Johnson & Borisy, 1977), but this ignores the possibility that they may reform under the assembly conditions.

(*d*) The property termed "dynamic instability" (Mitchison & Kirschner, 1984), in which individual microtubules under steady-state conditions can exhibit different behaviours as a result of the stochastic loss of a terminal 'GTP cap' such that subunits are lost at rates governed by $k_{-1}{}^{GTP}$ or $k_{-1}{}^{GDP}$ (Carlier *et al.*, 1984). The consequence of this effect is that the steady-state critical concentration exceeds that predicted ($C_0{}^{GTP}$) by the initial elongation kinetics. Dynamic instability is generally suppressed by MAPs (Horio & Hotani, 1986; Farrell *et al.*, 1987; Rothwell *et al.*, 1986; Bré & Karsenti, 1990).

(*e*) End-to-end annealing of microtubules (Rothwell *et al.*, 1986, 1987) such that the molar concentration of microtubule ends ([M]) decreases.

Finally, further restrictions apply when unfractionated microtubule protein, rather than pure tubulin, is studied as phosphorylation of the MAPs affects the assembly kinetics (Burns *et al.*, 1984). It is therefore necessary to develop an experimental strategy which either eliminates the above restrictions or limits their effects in a defined manner. As the precise conditions used to prepare microtubule protein can affect its polymerization properties (Karr & Purich, 1979), the chick brain MAP2–tubulin microtubule protein has been fully characterized under the selected buffer conditions, both before and after the analysed cycle of assembly. Particular attention has been paid to whether the composition of the microtubule protein and the extent of the post-translational modifications is altered during assembly, whether the assembled microtubules anneal, and whether they exhibit dynamic instability. This is the first time that all these properties have been simultaneously described for a single source of microtubule protein, and they form the framework for subsequent studies on the detailed analysis of the assembly and steady-state behaviour of MAP2–tubulin microtubules under conditions which do not permit the direct

Abbreviations and terms used: Tu^{GTP} or Tu^{GDP} describes tubulin dimers with GTP or GDP bound to the exchangeable site of the β-subunit; $k_{+1}{}^{GTP}$ and $k_{-1}{}^{GTP}$ are the association and dissociation rate constants for addition and loss of Tu^{GTP} tubulin dimers, and $k_{-1}{}^{GDP}$ is the dissociation rate constant for Tu^{GDP} subunits; $C_0{}^{GTP}$ is the critical concentration (or $k_{-1}{}^{GTP}/k_{+1}{}^{GTP}$) for assembly with GTP before the onset of dynamic instability, [M] the molar concentration of assembled microtubules, and c the assembly-competency of the protein; MAPs, microtubule-associated proteins.

addition of MAP2–tubulin oligomers [the accompanying papers (Burns, 1991; Symmons & Burns, 1991)].

MATERIALS AND METHODS

Preparation of microtubule protein

The microtubule protein was purified from 1-day-old chicks through two cycles of assembly and disassembly (Burns & Islam, 1981), except that leupeptin (10 $\mu g \cdot ml^{-1}$) was included in the homogenization buffer to inhibit MAP2 proteolysis, and 1 mM-ATP was used to promote assembly during the first cycle and 0.5 mM-GTP with 1 mM-phosphoenolpyruvate and pyruvate kinase (6 $\mu g \cdot ml^{-1}$) during the second cycle. The cold dissociation step after the second cycle of assembly was extended to 2 h to permit the full dephosphorylation of the MAP2 (see the Results section for details). The assembly buffer consisted of 100 mM-Mes/2.5 mM-EGTA/1 mM-dithiothreitol/0.5 mM-$MgCl_2$/0.1 mM-EDTA (adjusted to pH 6.4 with KOH). The NaCl-supplemented buffer was identical, except that 67 mM-NaCl was included.

Analytical methods

Proteins were fractionated by SDS/PAGE (Laemmli, 1970) on 6% or 8% (w/v) acrylamide tube gels. The gels were stained with Coomassie Blue G-250 (Fairbanks *et al.*, 1971) and destained with 10% (v/v) acetic acid.

Proteins were fractionated by isoelectric focusing on a 16 cm × 16 cm × 0.1 cm slab gel, consisting of 4% acrylamide, 0.23% bisacrylamide, 9 M-urea, 2% Nonidet P40, 0.8% pH 4–6 and 0.2% pH 5–7 Ampholines, 0.15 M-Bicine, 0.001% *NNN'N'*-tetramethylethylenediamine and 0.02% ammonium persulphate. The anode buffer was 20 mM-phosphoric acid and the cathode buffer 0.2 M-NaOH. The gels were pre-run at 8 W for 30 min and, after loading of the protein samples, were run at 10 W for 6 h with cooling. The gels were stained with 0.1% Coomassie Blue G-250 in methanol/acetic acid/water (5:1:4, by vol.) destained in the same solution, and stored in 10% (v/v) acetic acid. The α- and β-tubulins were identified by immunoblotting with monomer-specific monoclonal antibodies (α-tubulin: YOL 1/34; Kilmartin *et al.*, 1982; β-tubulin: KMX; Birkett *et al.*, 1985).

Protein concentrations were measured (Hartree, 1972) with BSA as standard. Protein concentrations were expressed both in terms of $mg \cdot ml^{-1}$ and μM-tubulin dimer, the latter being calculated from the total protein content and the observation that 80% of it is tubulin (Burns, 1990).

Protein fractionation

Pure tubulin was prepared as the void fraction on elution of twice-cycled microtubule protein through a 0.9 cm × 10 cm phosphocellulose column equilibrated with the unmodified assembly buffer. The microtubule protein was also fractionated at 4 °C or 37 °C, with or without prior fixation with 0.1% glutaraldehyde, on a 28 cm × 0.9 cm Bio-Gel A15m column to characterize the oligomers, or through a 28 cm × 0.9 cm column of Sephadex G-50 (Pharmacia), equilibrated with the NaCl-supplemented assembly buffer, to remove the exogenous nucleotide.

MAP2 phosphorylation

The stoichiometry of MAP2 phosphorylation was determined as previously described (Islam & Burns, 1981; Burns & Islam, 1984). The protein was labelled with [γ-^{32}P]GTP, fractionated by SDS/PAGE, after which the gels were sliced and counted for radioactivity, and the stoichiometries calculated from the protein content and the incorporation relative to the initial inputs.

Kinetics of microtubule assembly

The void fraction eluted from the Sephadex G-50 column (generally 2–2.5 $mg \cdot ml^{-1}$; 16–20 μM-tubulin) was adjusted to 100 μM-GTP, 1 mM-phosphoenolpyruvate and pyruvate kinase (60 $\mu g \cdot ml^{-1}$), degassed, and transferred to warmed cuvettes in a Beckman DU-8 spectrophotometer fitted with temperature-controlled cuvettes. The kinetics at 37 °C were monitored by measuring the turbidity at A_{350} and its rate of change. For analysis of dynamic instability and annealing, microtubule protein (2 $mg \cdot ml^{-1}$, 16 μM-tubulin) was assembled to steady state with 100 μM-GTP and a GTP-regenerating system, sheared by ten passages through a 100 μl Hamilton syringe, and incubated for increasing times at 37 °C. Samples were fixed with 0.1% glutaraldehyde in the appropriate buffer, negatively stained with 1% uranyl acetate, and viewed with a JEM 1200-EX electron microscope. Microtubules, selected solely on the basis of the quality of the negative staining, were photographed (5000–10000 ×). The mean lengths were determined by measuring each microtubule on the negative, doubling the lengths of those which extended beyond the edge of the negative (Johnson & Borisy, 1977).

Materials

All biochemicals were purchased from Sigma Chemical Co., phosphocellulose was from Whatman, Bio-Gel A15m was from Bio-Rad Laboratories, [γ-^{32}P]GTP was from Amersham International, and the YOL1/34 monoclonal antibody and secondary antibodies were from Serotech Ltd. All other materials were of the highest grades available.

RESULTS

The microtubule protein

The composition of microtubule protein, purified through two cycles of assembly and disassembly, was examined in order to

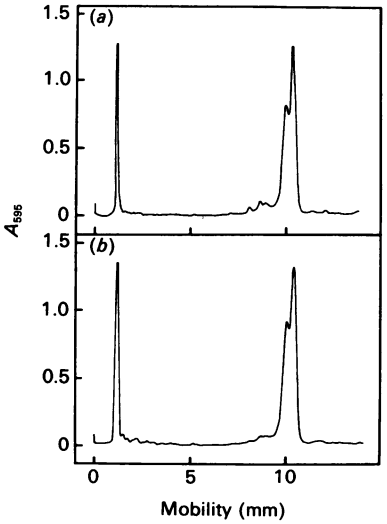

Fig. 1. Fractionation of microtubule protein by SDS/PAGE

(*a*) Microtubule protein purified through two cycles of assembly; (*b*) the pelleted microtubules (100000 *g*, 30 min, 30 °C) after a third cycle of assembly in the NaCl-supplemented buffer with 500 μM-GTP. The proteins were fractionated on a 8%-polyacrylamide gel, stained with Coomassie Blue, destained, and scanned at A_{595}. The principle peaks are MAP2 and α- and β-tubulin, with the tau components running immediately behind the tubulin bands.

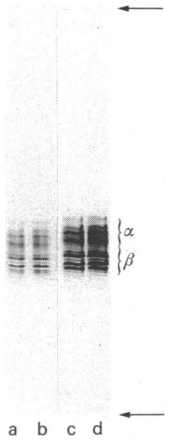

Fig. 2. Fractionation of tubulin by isoelectric focusing

a and c, Tubulin prepared from microtubule protein purified through two cycles of assembly and disassembly; b and d, the pelleted microtubules after a third cycle of assembly in the NaCl-supplemented buffer with 500 μM-GTP. The increased loadings of lanes c and d show the presence of additional minor components. The tubulin was prepared by fractionation on a phosphocellulose column equilibrated with the unmodified assembly buffer, with the tubulin being eluted in the void fraction. Parallel lanes were immunoblotted with YOL34 and KMX monoclonal antibodies to identify respectively the α- and β-tubulin isoforms (results not shown). The top and bottom of the gel are marked with arrows.

establish whether the composition is altered by a further cycle of assembly, and to identify buffer conditions which minimize any such changes. Fractionation of the protein on SDS/8%-polyacrylamide gels typically shows that it contains tubulin and MAP2, with trace amounts of the 320000–380000-M_r MAP1 isoforms and the tau components (Fig. 1*a*). MAP2 is the sharp band towards the top of the gel, whereas α- and β-tubulin are the predominant and partially resolved bands. The minor bands running immediately behind the tubulin, and which vary between microtubule preparations, include the tau components. Various identified enzymic activities are also present, including phosphoprotein phosphatase(s) (Islam & Burns, 1981), nucleoside diphosphate kinase (0.25 units·mg^{-1} for the twice-cycled protein; Islam & Burns, 1985), and the catalytic subunit of the cyclic AMP-activated protein kinase (see, e.g., Islam & Burns, 1981); the regulatory subunit is absent from protein prepared at pH 6.4 (Burns & Islam, 1986).

The tubulin, after removal of the MAPs by phosphocellulose chromatography, can be separated by isoelectric focusing into 10–11 β-tubulin isoforms and a similar number of α-tubulins (Figs. 2, a and c). The profile closely resembles that reported previously for chick brain tubulin (Sullivan & Wilson, 1984).

Only a single MAP2 is detected by SDS/PAGE (Fig. 1*a*), even though mammalian brain contains two such MAP2 isoforms, which vary in amount during development (Binder *et al.*, 1984). All attempts to separate the chick MAP2 into distinct isoforms were unsuccessful (results not shown).

As phosphorylation of MAP2 by the cyclic AMP-activated protein kinase affects its ability to promote microtubule assembly (Jameson & Caplow, 1981; Burns *et al.*, 1984), it has been important to establish the level of this phosphorylation before and after the additional cycle of assembly. Once-cycled microtubule protein was assembled with 500 μM-[^{32}P-γ]GTP in the presence or absence of 20 mM-NaF, to inhibit the co-purifying phosphoprotein phosphatases, and then fractionated by SDS/PAGE. Protein, labelled in the presence of NaF and analysed after pelleting but before the cold dissociation, was phosphorylated to 2.3 mol·mol^{-1}, whereas protein labelled without NaF was phosphorylated to 1.2 mol·mol^{-1}. After the 2 h cold dissociation and clarification, the stoichiometries had fallen to 2.0 and 0.8 mol·mol^{-1} respectively.

The once-cycled microtubule protein therefore contains sufficient phosphoprotein phosphatase activity to remove almost all the phosphates incorporated during the second cycle of assembly. This incorporation was by the cyclic AMP-activated protein kinase, since the buffer conditions preclude labelling by either the Ca^{2+}/calmodulin-dependent (Goldenring *et al.*, 1985) or the Ca^{2+}/phospholipid-dependent (Tsuyama *et al.*, 1986) protein kinases. Protein labelled during the third cycle of assembly could not be fully dephosphorylated by the endogenous phosphoprotein phosphatases (results not shown), and this accounts for the selection of twice-cycled microtubule protein for further analysis.

This twice-cycled protein will be referred to as being 'unphosphorylated', since although the absolute level of phosphorylation of MAP2 is unknown, almost all the residues phosphorylated by the co-purifying protein kinase(s) are dephosphorylated during the subsequent cold-dissociation step by the co-purifying phosphoprotein phosphatases.

MAP2–tubulin oligomers

A variety of buffers were examined for their ability to dissociate the MAP2–tubulin oligomers, to promote the assembly of MAP2–tubulin microtubule protein, but not to permit the assembly of tubulin purified by either DEAE-cellulose or phosphocellulose chromatography. The selected buffer consists of the assembly buffer supplemented with 67 mM-NaCl; preliminary studies showed that the oligomers were not fully dissociated at lower ionic strengths, whereas the addition of more than 75 mM-NaCl affected the rate of microtubule assembly (R. G. Burns, unpublished work). Pure tubulin ($\geqslant 40$ μM, or concentrations about twice those routinely used for studying the assembly of the unfractionated protein) failed to assemble in this NaCl-supplemented buffer, even when seeded. Four independent lines of evidence suggest that the MAP2–tubulin oligomers are not direct assembly intermediates under these buffer conditions.

Gel filtration. Unassembled microtubule protein in either the unmodified or the NaCl-supplemented buffer was fixed with 0.1% glutaraldehyde at 4 °C and fractionated on a Bio-Gel A15m column (Fig. 3). Similar profiles were observed on fractionation of glutaraldehyde-fixed protein which had first been warmed to 37 °C in the absence of added GTP. The protein in the unmodified buffer shows peaks eluted in the void volume (fraction 7), with a k_d of $\simeq 0.45$ (fractions 9–10), and in the salt volume (fractions 13–15). By contrast, almost all the protein in the NaCl-supplemented buffer was eluted in the salt volume (fractions 13–15). Similar profiles were observed without prior fixation, and SDS/PAGE of such protein confirmed that the major peak in the NaCl-supplemented buffer consists of tubulin, with MAP2 being eluted on the leading edge. By contrast, the k_d-0.45 peak observed with the unmodified buffer contains both tubulin and MAP2, indicating that it is an oligomeric complex.

Nucleation kinetics. When the assembly of microtubule assembly in the unmodified buffer is monitored by turbidity, a small decrease is frequently observed before the rapid increase associated with microtubule assembly (see, e.g., Bayley *et al.*, 1985). This temperature-dependent decrease has been attributed to the partial dissociation of the rings to 'unrolled' protofilaments, which are then added to the elongating microtubule (Bordas *et al.*, 1983). This initial decrease is never

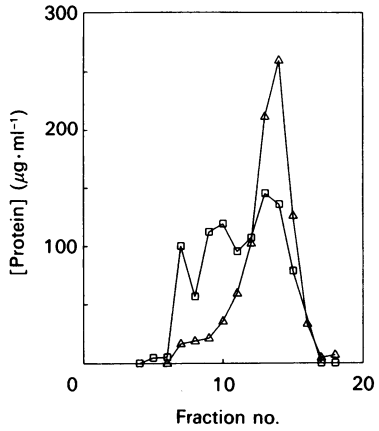

Fig. 3. Gel filtration of microtubule protein on a Bio-Gel A15m column

□, Twice-cycled microtubule protein fixed with 0.1% glutaraldehyde and fractionated on a 28 cm × 0.9 cm Bio-Gel A15m column equilibrated with the unmodified assembly buffer. △, Twice-cycled microtubule protein adjusted to 67 mM-NaCl, fixed with 0.1% glutaraldehyde and fractionated on the same column after equilibration with the NaCl-supplemented assembly buffer. The protein concentrations of each fraction are shown.

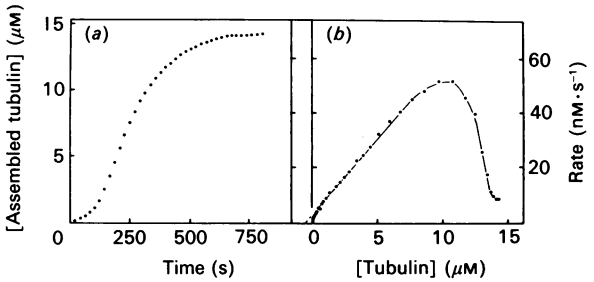

Fig. 4. Kinetics and analysis of microtubule assembly

(*a*) Assembly of twice-cycled microtubule protein (2.1 mg·ml^{-1}, 17 μM-tubulin) with 500 μM-GTP in the NaCl-supplemented assembly buffer at 37 °C. The increase in turbidity at A_{350} is expressed as μM-tubulin assembled, using the coefficient that 1 A unit is equivalent to 44 μM assembled tubulin. (*b*) The kinetics shown in (*a*) re-expressed as the instantaneous rate of polymer formation (nM·s^{-1}) versus the concentration of free tubulin dimer yet to be assembled, i.e. A_{350} at steady state − A_{350} at time t, expressed in μM-tubulin. This analysis eliminates any requirement to consider concomitant disassembly of the microtubules (determined by k_{-1}[M]) and compensates for any assembly-incompetent protein. Steady state is achieved when the unassembled tubulin concentration falls to 0 μM: early time points of the assembly profile lie to the right of the Figure.

observed with protein in the NaCl-supplemented buffer, indicative of the absence of the MAP2–tubulin oligomers.

Elongation kinetics. The assembly kinetics of unfractionated microtubule protein in the unmodified assembly buffer are complex, in that a plot of the instantaneous rate of assembly as a function of the concentration of subunits yet to be assembled is biphasic (see, e.g., Burns & Islam, 1986). These biphasic kinetics indicate the direct incorporation of both tubulin dimers and MAP2–tubulin oligomers during the initial stages of elongation, whereas only tubulin dimers are added as assembly approaches steady state.

Microtubule protein was assembled with 500 μM-GTP in the NaCl-supplemented buffer (Fig. 4*a*). The general form of the assembly curve is similar to that under other assembly conditions,

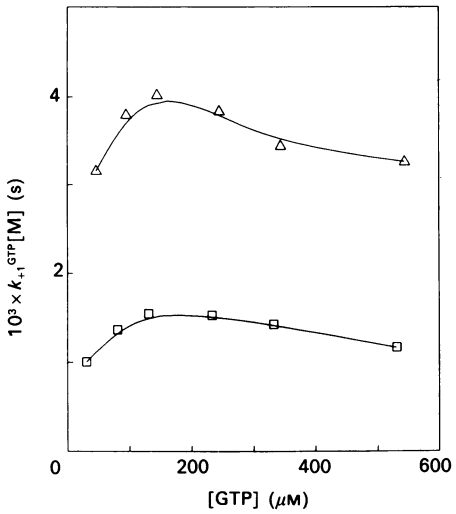

Fig. 5. Kinetics of microtubule assembly as a function of the GTP concentration

Twice-cycled microtubule protein (□, 1.6 mg·ml^{-1}, 12.75 μM-tubulin; △, 1.08 mg·ml^{-1}, 8.5 μM-tubulin) was assembled in the NaCl-supplemented assembly buffer with increasing GTP concentrations. The calculated pseudo-first-order rate constants (k_{+1}^{GTP}[M]) were plotted against the concentration of added GTP.

with a short nucleation phase followed by rapid elongation towards steady state. The precise kinetics are more evident from a plot of the instantaneous rate of assembly versus the concentration of subunits yet to be assembled (Fig. 4*b*), calculated from the difference in turbidity at time t compared with that at steady state. This instantaneous rate increased sharply during nucleation (i.e. at the right), and was then proportional to the concentration of subunits yet to be assembled into microtubules, until shortly before the attainment of steady state, at which time the rate of assembly sharply declined (i.e. towards the origin). The slope of this plot equals the pseudo-first-order rate constant (k_{+1}^{GTP}[M]). The kinetics are significantly different from those observed when the MAP2–tubulin oligomers can directly participate in microtubule assembly (see, e.g., Islam & Burns, 1986; Barton *et al.*, 1987), since the instantaneous rate of assembly immediately before steady state if greater than that predicted from the initial elongation kinetics when 67 mM-NaCl is omitted.

Effect of the GTP concentration. The value of K_{+1}^{GTP}[M], determined from the initial elongation kinetics, is markedly dependent upon the GTP concentration under conditions which permit the direct addition of MAP2–tubulin oligomers, and this effect has been attributed to GTP affecting the efficiency of oligomer addition (Burns & Islam, 1984; Islam & Burns, 1986). By contrast, the value of k_{+1}[M] in the NaCl-supplemented buffer at two protein concentrations is essentially independent of the added GTP concentration (Fig. 5), with a maximum at about 100 μM-GTP and a slight inhibition at high GTP concentrations.

Changes induced by microtubule assembly

Protein composition. Twice-cycled microtubule protein was assembled with 500 μM-GTP at 37 °C and, after pelleting, the assembled proteins were fractionated by SDS/PAGE and by isoelectric focusing (Figs. 1*b* and Fig. 2, b and d). Comparison of the gels with those of twice-cycled microtubule protein shows no significant differences. In particular, the MAP2 stoichiometry is unaltered (Figs. 1*a* and 1*b*), whereas there is no qualitative or quantitative difference in the tubulin isoform pattern (Fig. 2).

There is, however, selective loss of certain of the co-purifying enzymic activities, including nucleoside diphosphate kinase and the phosphoprotein phosphatase(s).

Post-translational modifications. Phosphocellulose-purified tubulin after the third cycle of assembly is indistinguishable from that after the second cycle (Fig. 2). Consequently there is no selective utilization of any of the isotypes, nor any evidence for dephosphorylation, deacetylation, or deglutamylation under the assembly conditions. Similarly, preliminary work using the anti-tyrosinylated α-tubulin monoclonal antibody (YL1/2; Wehland *et al.*, 1983) shows no selective loss of the tyrosinylated form during the third cycle of assembly.

The kinetics of MAP2 phosphorylation during GTP-induced assembly in the NaCl-supplemented buffer have also been examined. Microtubule protein was assembled in the NaCl-supplemented assembly buffer at 37 °C with 100 μM- or 500 μM-[γ-^{32}P]GTP for increasing times, and then fractionated by SDS/PAGE to measure the specific activity of MAP2. The phosphorylation kinetics resemble those in the unmodified buffer (Burns & Islam, 1984), although the extent of labelling was lower (Fig. 6), possibly due to the added NaCl affecting the protein kinase–MAP2 interaction or to the omission of NaF, previously included to inhibit partially phosphoprotein phosphatase activity. MAP2 phosphorylation increased in 60 min to $\simeq$ 0.7 mol·mol^{-1} on incubation with 100 μM-GTP and to about 2 mol·mol^{-1} with 500 μM-GTP. There is therefore minimal phosphorylation ($\leqslant$ 1 mol·mol^{-1}) by either 100 or 500 μM-GTP during the usual time course for assembly (10–15 min). Such a low level of phosphorylation has a minimal effect on the assembly kinetics (Burns *et al.*, 1984), so that the kinetic analysis of microtubule assembly can largely ignore the effects of any concomitant phosphorylation.

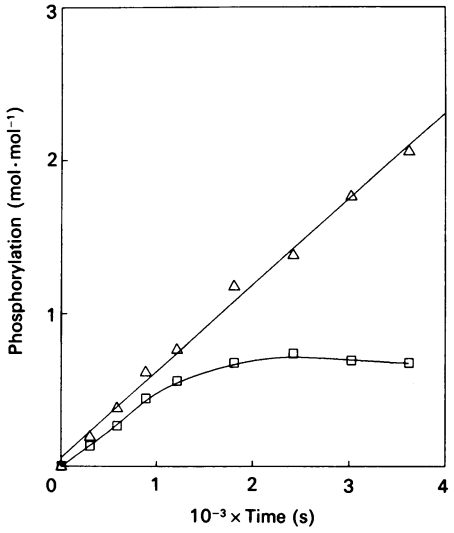

Fig. 6. Kinetics of MAP2 phosphorylation of twice-cycled microtubule protein in the NaCl-supplemented assembly buffer by 100 μM-(□) or 500 μM-(△) [^{32}P-γ]GTP

Microtubule protein (2.0 mg·ml^{-1}; 16 μM-tubulin) was incubated for increasing times with 100 or 500 μM-[^{32}P-γ]GTP, fractionated on SDS/6% polyacrylamide gels, which were stained, scanned, sliced and counted to determine the specific radioactivity of the MAP2.

Dynamic instability and annealing

Twice-cycled microtubule protein was assembled with 500 μM-GTP and a GTP-regenerating system to steady state in the unmodified Mes assembly buffer, diluted with this buffer or adjusted to 67 mM-NaCl, and incubated for a further 20 min to permit steady state to be regained. On shearing, the microtubules in the Mes assembly buffer exhibited minimal length redistribution (Figs. 7*a* and 7*b*), having an initial mean length of 0.74 μm (±0.49 μm, n = 306), and a mean length after 5 min of 1.17 μm (±0.82, n = 320). By contrast, the microtubules in the NaCl-supplemented buffer increased in 5 min from 1.03 μm (±0.59 μm, n = 272) to a mean length of 3.14 μm (n = 211; Figs. 7*c* and 7*d*). Calculation of the S.D. for microtubules exhibiting dynamic instability is not applicable, partly because the microtubules no longer belong to a single Gaussian population, and partly because the mean lengths were calculated by doubling the lengths of any microtubules overlapping the margins of the micrographs (see the Materials and methods section).

The enhanced length redistribution in only the NaCl-supplemented buffer suggests that it is due to dynamic instability rather than to end-to-end reannealing. This was tested in two ways. First, microtubule protein was assembled, sheared, and then a fixed volume of the sheared (20 μl, mean length 1.45 μm) microtubules was diluted with increasing volumes of the microtubule protein at the C_0 (the supernatant remaining after pelleting the preassembled microtubules at 100000 *g* for 5 min at 20 °C). The increase in the mean lengths observed after 150 s was least in the samples containing the highest initial concentration of microtubule ends (Fig. 8), demonstrating that the length redistribution was independent of [M] and therefore not due to end-to-end reannealing. The higher rate of length redistribution

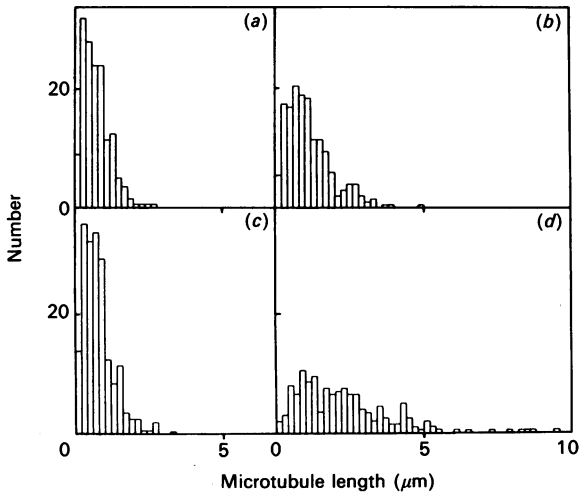

Fig. 7. Length redistribution of sheared microtubules in either the unmodified (*a* and *b*) or the NaCl-supplemented assembly buffer (*c* and *d*)

Microtubule protein (2.0 mg·ml^{-1}; 16 μM-tubulin) was assembled to steady state in the unmodified assembly buffer with 500 μM-GTP and a GTP-regenerating system. The microtubules were either diluted with this buffer or adjusted to 67 mM-NaCl and incubated for a further 20 min at 37 °C before shearing. (*a*) and (*c*) Immediately after shearing; (*b*) and (*d*), after incubation at 37 °C for 300 s.

with the greater dilution was probably due to the concentration of assembly-competent protein exceeding the steady-state critical concentration by $\simeq$ 0.3 μM-tubulin dimer, possibly due to some microtubules dissociating during the preparatory centrifugation spin at ambient temperature.

Secondly, when microtubules were assembled in the NaCl-supplemented buffer, sheared and then incubated with demembranated *Tetrahymena* axonemes, the sheared fragments

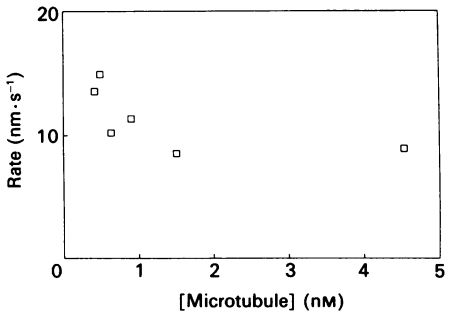

Fig. 8. Rate of length redistribution as a function of the microtubule concentration

Microtubule protein (2.65 mg·ml^{-1}; 21.2 μM-tubulin) was assembled to steady state with 100 μM-GTP and a GTP-regenerating system, and then sheared. These microtubules were diluted into various volumes of microtubule protein at the C_0 and incubated at 37 °C for a further 150 s. The C_0 protein was prepared by assembling microtubule protein to steady state as described above, pelleting the assembled microtubules (100000 *g*, 10 min, ambient temperature) and using the supernatant to dilute the sheared microtubules.

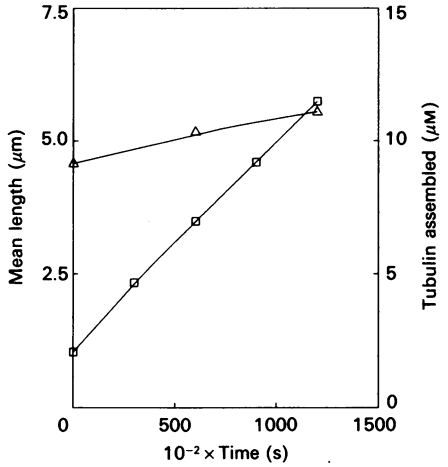

Fig. 9. Time course of the length redistribution of sheared microtubules (□) and protein content (△)

Microtubule protein (1.94 mg·ml^{-1}; 15.5 μM-tubulin) was assembled to steady state with 100 μM-GTP and a GTP-regenerating system, sheared, and incubated at 37 °C. Samples were removed for length measurements or for determination of the amount of assembled protein (100000 *g*, 3 min).

did not become associated with the axonemal microtubules. This contrasts with the observation for pure tubulin microtubules (Caplow *et al.*, 1986).

The redistribution under these conditions was therefore further examined by assembling microtubule protein to steady state, shearing, and removing samples for length measurement and for pelleting to determine the protein content. There is an approximately linear increase in the mean length over a 20 min period at 37 °C with minimal net microtubule assembly (Fig. 9). The amount of pelleted protein increased by approx. 15% within the first 10 min, and by a further 7% by 20 min. The former probably represents in part net addition to the sheared microtubules, whereas the latter is largely due to the aggregation of the assembly-incompetent protein. Calculation of the microtubule number concentration shows a progressive decline, that is, some microtubules are becoming totally disassembled, whereas others continue to elongate. Consequently, the minimal requirement of dynamic instability, length redistribution under steady-state conditions, is satisfied.

DISCUSSION

The properties of chick brain microtubule protein have been described, both before and after the third cycle of assembly in a buffer supplemented with 67 mM-NaCl. This description has been necessary to avoid, in any subsequent analysis of the assembly kinetics, having to extrapolate from studies of either pure tubulin or unfractionated microtubule protein prepared or analysed under different conditions or from different sources.

The chick brain microtubule protein consists essentially of a stoichiometric mixture of MAP2 and tubulin (Fig. 1). Its simple composition, which is a direct consequence of the homogenization and buffer conditions (Burns, 1990), makes it ideal for the subsequent kinetic studies. It is unaltered, apart from minimal phosphorylation (Fig. 6), by the third cycle of assembly, so that the precondition for treating microtubule assembly and disassembly as equilibrium reactions is satisfied.

Conditions have been identified which result in the dissociation of the MAP2–tubulin oligomers, but which still permit microtubule assembly (Figs. 3–5). Indeed, as the MAP2–tubulin stoichiometry remains unaltered (Fig. 1), and there is no assembly of pure tubulin, the observed assembly in the NaCl-supplemented buffer reflects the MAP2-directed addition and loss of tubulin dimers. Furthermore, the length redistribution of sheared steady-state microtubules is due to dynamic instability and not to end-to-end annealing (see below). This experimental system is therefore ideal for studying the kinetic properties of MAP2–tubulin microtubules and for comparing these properties with those described for pure tubulin microtubules.

The simplicity of the observed kinetics (Fig. 4*b*) permits the extraction of considerable information from the plot of the instantaneous rate of increase in turbidity versus the remaining concentration of subunits yet to be assembled. This use of the difference between the amount of assembly at time t and that at steady state represents an important innovation. Substituting $C_0^{GTP} \cdot k_{+1}^{GTP}$ for k_{-1}^{GTP} in the equation describing the linear condensation model together with a term, c, defining the assembly competency of the protein yields:

$$-\mathrm{d[Tu]}/\mathrm{d}t = k_{+1}^{GTP}[\mathrm{M}](c[\mathrm{Tu}] - C_0^{GTP})$$

Consequently, a plot (see, e.g., Fig. 4*b*) of the instantaneous rate versus the concentration of subunits yet to be assembled (c[Tu] − C_0^{GTP}) yields a direct estimation of the pseudo-first-order rate constant, k_{+1}^{GTP}[M]. The linearity of this plot between the end of nucleation and shortly before steady state confirms the independent demonstration (Fig. 8) that there is either no, or only minimal, reannealing.

This pseudo-first-order rate constant is generally obtained by plotting ln(assembly$^{steady\ state}$ − assembly^{t}) versus time (t). Such plots are generally non-linear, owing to an underestimation of the extent of assembly at steady state, resulting form the increase in the critical concentration after the onset of dynamic instability (Mitchison & Kirschner, 1984; Walker *et al.*, 1988). The approach described here eliminates this non-linearity by assigning the change in the critical concentration to the non-linear portion close to the intercept. Indeed, this pseudo-first-order plot can be used to predict the extent of assembly that would be attained at steady state in the absence of any dynamic instability. Extrapolation of this plot to the abscissa yields an estimate of the difference between the predicted and observed extents, i.e. to the difference caused by the change in the dissociation rate constant resulting from the assembly-dependent GTP hydrolysis.

Many studies have determined the initial rate of assembly as a function of the initial protein concentration in order to determine k_{+1}^{GTP}. Such measurements are difficult, for the following reasons.

(*a*) The rate of elongation decreases with time, with the maximum rate off a single microtubule occurring immediately after nucleation. Nucleation is not an instantaneous event in bulk solution, so that the maximum rate of elongation is only observed after nucleation has essentially ended, with the effect that the initial rate of elongation is underestimated.

(*b*) The turbidity is only proportional to the mass of polymer if the assembled polymers have similar, and unchanging, geometries (Berne, 1974). This does not apply to the earliest stages of microtubule assembly, with the effect that turbidity measurements tend to underestimate the initial extent of microtubule polymerization.

(*c*) The method generally used to determine k_{+1}^{GTP} has been to measure the initial rate of assembly off exogenous seeds as a function of the initial subunit concentration (see, e.g., Johnson & Borisy, 1977). This method, already subject to the criticisms above, further assumes that there is no self-nucleation, i.e. that the increase in turbidity is due solely to elongation off the exogenous seeds and that the protein is fully assembly-competent.

The pseudo-first-order plot (e.g. Fig. 4*b*) avoids these specific problems, since the slope is determined from data obtained during much of the elongation phase. In particular, the problems derived from the changing geometry of the polymer are avoided as its length during the rapid phase of elongation is generally considerably greater than the wavelength used (350 nm). Consequently, the use of data derived after nucleation to determine $k_{+1}^{GTP}[M]$ permits the accurate determination of k_{+1}^{GTP} from the change in $k_{+1}^{GTP}[M]$ as a function of the exogenous seed concentration (Burns, 1991; Symmons & Burns, 1991). Furthermore, it has the further advantage of directly compensating for the assembly-competency of the protein.

This pseudo-first-order plot is only valid when elongation is effected by the addition and loss of a single molecular species to the microtubule end, and it cannot be used to analyse the kinetics of assembly from a mixture of tubulin dimers and MAP2–tubulin oligomers.

The assembled microtubules exhibit length redistribution (Figs. 7 and 9). This is not due to annealing, since observed redistribution is dependent upon the number concentration of microtubule ends (Fig. 8). This was also reported for the reannealing of pure tubulin microtubules by Rothwell *et al.* (1986, 1987), who proposed that the apparent independence was due to the parallel alignment of the longer microtubules such that the ends were not freely available for reannealing. Indeed, comparison of the efficiency of reannealing of pure tubulin microtubules assembled under apparently similar conditions showed $\simeq 10\%$ reannealing in 3 h for 14 μm microtubules (Kristofferson *et al.*, 1986) compared with $> 70\%$ in 1 h for 1 μm fragments (Rothwell *et al.*, 1987). This length effect cannot account for the present results, since no length redistribution was observed when the microtubules were assembled and sheared in buffer lacking the supplementary NaCl (Fig. 7). Furthermore, no capture of sheared microtubules by *Tetrahymena* axonemes has been detected. It therefore seems likely that there is no significant reannealing in the NaCl-supplemented assembly buffer, and that the observed length redistribution is due to dynamic instability. Indeed, as the MAP2 molecules form projecting sidearms on the microtubule surface (see, e.g., Voter & Erickson, 1982), they may prevent the required side-by-side alignment of the microtubules. Although MAPs markedly inhibit dynamic instability under other buffer conditions (Horio & Hotani, 1986; Farrell *et al.*, 1987; Rothwell *et al.*, 1986; Bré & Karsenti, 1990), the inclusion of 67 mM-NaCl weakens the MAP2–microtubule interaction sufficiently to permit dynamic instability while continuing to permit the MAP2-dependent addition of tubulin dimers.

In summary, the chick brain MAP2–tubulin microtubule protein, assembled in the NaCl-supplemented buffer, is ideal for testing the detailed kinetics of microtubule assembly in that the protein, isotype and phosphorylation status are unchanged by the assembly, the kinetics conform (until shortly before steady state) with the predictions of the linear condensation theory, and the microtubules exhibit dynamic instability but minimal reannealing.

I thank Ross Breeders Ltd. for generously donating the chicks, Professor K. Gull for the KMX monoclonal antibody, and the Science and Engineering Research Council for their support.

REFERENCES

Arce, C. A. & Barra, H. S. (1983) FEBS Lett. **157**, 75–78
Barton, J. S., Vandivort, D. L., Heacock, D. H., Coffman, J. A. & Trygg, K. A. (1987) Biochem. J. **247**, 505–511
Bayley, P. M., Butler, F. M. M., Clark, D. C., Manser, E. J. & Martin, S. R. (1985) Biochem. J. **227**, 439–455
Berne, B. J. (1974) J. Mol. Biol. **89**, 755–758
Binder, L. I., Frankfurter, A., Kim, H., Caceres, A., Payne, M. R. & Rebhun, L. I. (1984) Proc. Natl. Acad. Sci. U.S.A. **81**, 5613–5617
Birkett, C. R., Foster, K. E., Johnson, L. & Gull, K. (1985) FEBS Lett. **187**, 211–218
Bordas, J., Mandelkow, E.-M. & Mandelkow, E. (1983) J. Mol. Biol. **164**, 89–135
Bré, M. H. & Karsenti, E. (1990) Cell Motil. Cytoskeleton **15**, 88–98
Burns, R. G. (1990) Cell Motil. Cytoskeleton **17**, 167–173
Burns, R. G. (1991) Biochem. J. **277**, 239–243
Burns, R. G. & Islam, K. (1981) Eur. J. Biochem. **117**, 515–519
Burns, R. G. & Islam, K. (1984) Biochem. J. **224**, 623–627
Burns, R. G. & Islam, K. (1986) Ann. N.Y. Acad. Sci. **466**, 340–356
Burns, R. G., Islam, K. & Chapman, R. (1984) Eur. J. Biochem. **141**, 609–615
Caplow, M., Shanks, J. & Brylawski, B. P. (1986) J. Biol. Chem. **261**,
Carlier, M.-F., Hill, T. L. & Chen, Y.-D. (1984) Proc. Natl. Acad. Sci. U.S.A. **81**, 771–775
Cleveland, D. W. & Sullivan, K. W. (1985) Annu. Rev. Biochem. **54**, 331–365
Cote, R. H. & Borisy, G. G. (1981) J. Mol. Biol. **150**, 577–602
Eddé, B., Rossier, J., Le Caer, J.-P., Desbruyeres, E., Gros, F. & Denoulet, P. (1990) Science **247**, 83–85
Erickson, H. P. (1974) J. Supramol. Struct. **2**, 393–411
Fairbanks, G., Steck, L. & Wallach, D. F. H. (1971) Biochemistry **10**, 2606–2617
Farrell, K. W., Jordan, M. A., Miller, H. P. & Wilson, L. (1987) J. Cell Biol. **104**, 1035–1046
Goldenring, J. R., Vallano, M. L. & DeLorenzo, R. J. (1985) J. Neurochem. **45**, 900–905
Hartree, E. F. (1972) Anal. Biochem. **48**, 422–427
Horio, T. & Hotani, H. (1986) Nature (London) **321**, 605–607
Islam, K. & Burns, R. G. (1981) FEBS Lett. **123**, 181–185
Islam, K. & Burns, R. G. (1985) Biochem. J. **232**, 651–656
Islam, K. & Burns, R. G. (1986) Ann. N.Y. Acad. Sci. **466**, 639–641
Jameson, L. & Caplow, M. (1981) Proc. Natl. Acad. Sci. U.S.A. **78**, 3413–3417
Johnson, K. A. & Borisy, G. G. (1977) J. Mol. Biol. **117**, 1–31
Karr, T. L. & Purich, D. L. (1979) J. Biol. Chem. **254**, 10885–10888
Kilmartin, J. B., Wright, B. & Milstein, C. (1982) J. Cell Biol. **93**, 576–582
Kirschner, M. W., Williams, R. C., Weingarten, M. & Gerhart, J. C. (1974) Proc. Natl. Acad. Sci. U.S.A. **71**, 1159–1163
Kristofferson, D., Mitchison, T. & Kirschner, M. (1986) J. Cell Biol. **102**, 1007–1019
Laemmli, U. K. (1970) Nature (London) **227**, 680–685
Margolis, R. L. & Wilson, L. (1978) Cell (Cambridge, Mass.) **13**, 1–8
Mitchison, T. & Kirschner, M. W. (1984) Nature (London) **312**, 237–242
Murphy, D. B., Johnson, K. A. & Borisy, G. G. (1977) J. Mol. Biol. **117**, 33–52

Pantaloni, D., Carlier, M.-F., Simon, C. & Batelier, G.. (1981) Biochemistry **20**, 4709–4716
Piperno, G. & Fuller, M. T. (1985) J. Cell Biol. **101**, 2085–2094
Rothwell, S. W., Grasser, W. A. & Murphy, D. B. (1986) J. Cell Biol. **102**, 619–627
Rothwell, S. W., Grasser, W. A., Baker, H. N. & Murphy, D. B. (1987) J. Cell Biol. **105**, 863–874
Scheele, R. B. & Borisy, G. G. (1978) J. Biol. Chem. **253**, 2846–2851
Sullivan, K. W. & Wilson, L. (1984) J. Neurochem. **42**, 1363–1371
Symmons, M. F. & Burns, R. G. (1991) Biochem. J. **277**, 245–253
Tsuyama, S., Bramblett, G. T., Huang, K.-P. & Flavin, M. (1986) J. Biol. Chem. **261**, 4110–4116
Voter, W. A. & Erickson, H. P. (1982) J. Ultrastruct. Res. **80**, 374–382
Walker, R. A., O'Brien, E. T., Pryer, N. K., Soboeiro, M. F., Voter, W. A., Erickson, H. P. & Salmon, E. D. (1988) J. Cell Biol. **107**, 1437–1448
Wandosell, F., Serrano, L., Hernandez, M. A. & Avila, J. (1986) J. Biol. Chem. **261**, 10332–10339
Wehland, J., Willingham, M. C. & Sandoval, I. V. (1983) J. Cell Biol. **97**, 1467–1475

Received 19 September 1990/11 January 1991; accepted 22 January 1991